Journal of Quantitative Spectroscopy & Radiative Transfer 131 (2013) 194–201

Contents lists available at ScienceDirect

Journal of Quantitative Spectroscopy & Radiative Transfer

journal homepage: www.elsevier.com/locate/jqsrt

Minimum principles in electromagnetic scattering by small aspherical particles

Alex B. Kostinski *, Ajaree Mongkolsittisilp

Department of Physics, Michigan Technological University, 1400 Townsend Drive, Houghton, MI 49931, USA

ARTICLE INFO

Article history:
Received 24 May 2013
Received in revised form
2 August 2013
Accepted 5 August 2013
Available online 14 August 2013

Keywords:
Electromagnetic scattering
Particle shape
Minimum principles

ABSTRACT

We consider the question of optimal shapes, e.g., those causing minimal extinction among all shapes of equal volume. Guided by the isoperimetric property of a sphere, relevant in the geometrical optics limit of scattering by large particles, we examine an analogous question in the low frequency approximation, seeking to disentangle electric and geometric contributions. To that end, we survey the literature on shape functionals and focus on ellipsoids, giving a simple discussion of spherical optimality for the coated ellipsoidal particle. Monotonic increase with asphericity in the low frequency regime for orientation-averaged induced dipole moments and scattering cross-sections is also shown. Additional physical insight is obtained from the Rayleigh–Gans (transparent) limit and eccentricity expansions. We propose connecting low and high frequency regimes in a single minimum principle valid for all size parameters, provided that reasonable size distributions of randomly oriented aspherical particles wash out the resonances for intermediate size parameters. This proposal is further supported by the sum rule for integrated extinction.

1. Introduction

The literature on light scattering by aspherical particles is vast, e.g., [1], ranging from radiative transfer, climatology and remote sensing of atmospheric aerosols [2,3] and microscopy of bacteria [4] to astrophysics of interstellar dust [5] and marine monitoring [6]. Any bounds that can be set on optimal shapes, not only provide insight but can also be of great utility. For example, in the geometrical optics limit, relevant to optically large particles, twice the geometric cross-section is a good approximation to the total extinction cross-section. Combined with a remarkable theorem, due to Cauchy, that orientation-averaged cross-sectional area of an ovaloid equals one-quarter of its surface area, the geometrical limit implies that spherical total cross-sections are always lower than those for any randomly oriented convex particles of equal volume. While perhaps not widely appreciated, this approximation was discussed in important papers in optics and atmospheric science [7,8]. The effect can be illustrated by considering spheroidal surface area, normalized by that of an equal volume sphere (denoted S_r), regarded as a function of the aspect ratio, e.g., see p. 620 of [9], given by $S_r=(1/2)(1-e^2)^{-1/3}+(1/4e)(1-e^2)^{2/3}\ln[(1+e)/(1-e)]$ where $e^2\equiv 1-(c/a)^2$ for oblate spheroids, and $S_r=(1/2)(1-e^2)^{1/3}+(1/2e)(1-e^2)^{-1/6}\sin^{-1}(e)$ where $e^2\equiv 1-(b/a)^2$ for prolate spheroids. The function, plotted in Fig. 1 vs. the aspect ratio ρ (curve labelled "geometric"), has a minimum at the spherical value of $\rho=1$. Note that the validity of the geometric limit, because of the optical theorem, is rather broader than might at first be expected [7].

The success of a simple geometric reasoning in the large particle limit prompted us to ask an analogous question for the small particle (low frequency) Rayleigh scattering regime. Here the physics of scattering is entirely different: governed by the magnitude of the induced

* Corresponding author. Tel.: +1 906 487 2580.
E-mail addresses: kostinsk@mtu.edu (A.B. Kostinski), amongkol@mtu.edu (A. Mongkolsittisilp).

0022-4073/$ - see front matter © 2013 Elsevier Ltd. All rights reserved.
http://dx.doi.org/10.1016/j.jqsrt.2013.08.006

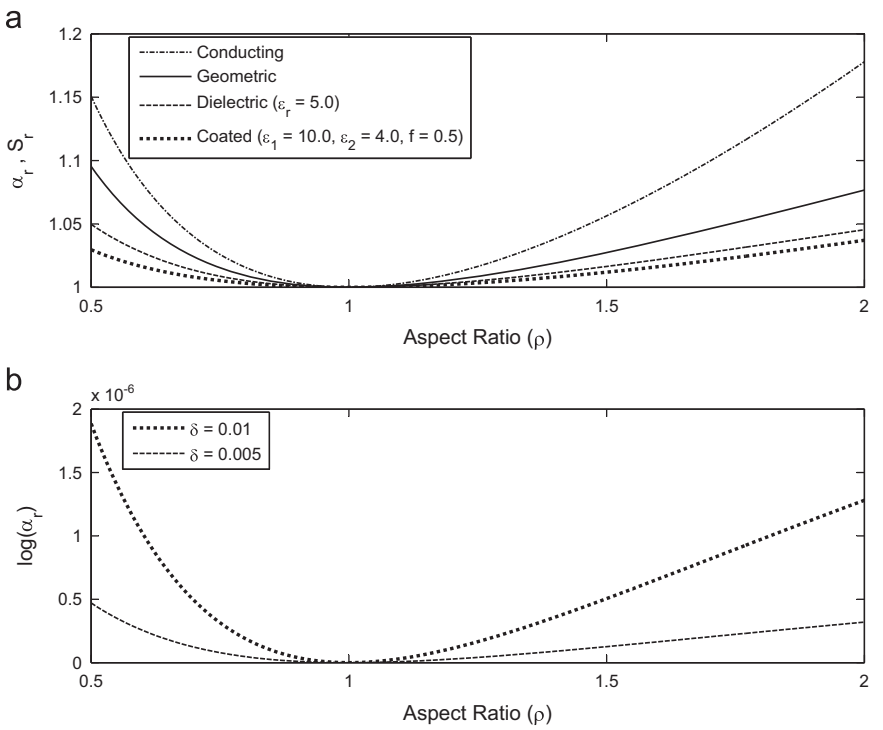

Fig. 1. Optimality of the spherical shape: polarizabilities. Top panel (a): Relative (normalized by the equal-volume-sphere value) surface area S_r (solid line), relative orientation-averaged polarizability (α_r) of conducting spheroids (dashed-dotted line), α_r of dielectric ellipsoids (dashed line), and α_r of confocal coated ellipsoid (dotted) vs. ρ, the aspect ratio. Bottom panel (b): Relative orientation-averaged polarizability of dielectric ellipsoids for two different values of the dielectric contrast δ (see text) in the Rayleigh–Gans (transparent) regime. The ordinate is the logarithm of the spherical access (see Eq. (11) in text). For both panels, oblate/prolate spheroids on left/right of unity.

dipole moment. Yet, the classical picture of a dielectric sphere placed in a uniform external electric field, resulting in the displaced net positive and negative charges on the opposing surfaces, evokes geometrical reasoning. Hence, we ask: do convex aspherical particles scatter more strongly than equivalent volume spheres? To render the question well posed, we further specify that the particles are randomly oriented and consider the magnitude of the orientation-averaged induced dipole moment. Thus, the question, apparently not raised before in the context of scattering theory, becomes: do randomly oriented convex aspherical particles (ovaloids) possess orientation-averaged magnitude of an induced dipole moment larger than that of equivalent volume spheres? By a way of preview, the answer is in the affirmative for a wide variety of circumstances. However, having conducted an extensive literature survey of related questions about particle shapes, we frequently encountered conflicting statements, scattered across a variety of disciplines.

For example, early influential developments in electromagnetics included statements such as one by Siegel [10, p. 294], *When the wavelength is much longer than the dimensions of a body, one cannot discern details of the structure of the body: the observed effect depends more on the size of the body than on its shape.* It is implied that, in the long wavelength regime, particle shape is not essential. Consider, for example, thermal IR remote sensing studies of aerosols which commonly ignore asphericity and model the scatterers by size-distributed Mie spheres, e.g., see pp. 1213–1214, Section 3.2, and data in Fig.11 of [11]. This is not a criticism as spherical modelling suffices for many purposes and authors in the field of atmospheric optics are well aware of the importance of asphericity, e.g., [2,3,12–16]. Yet, integral statements of shape optimality are rare in the small particle regime. Consider, for instance, an important and insightful recent review in this journal [17] where in the 2nd paragraph of the Abstract it is stated that "*for particles much smaller than the wavelength of incident light, absorption is proportional to the particle volume and mass*". This statement must be qualified by specifying particle shape. Otherwise, as discussed below, spheroids absorb and scatter more than equal-volume (mass) spheres.

Early literature in radar meteorology dealt with shape effects but only for the case of backscatter, e.g., [18], concluding numerical calculations with the conjecture that spheroids do have larger echoes than equal volume spheres. In applied optics, the question of optimal shape for absorption in the visible was tackled almost at the same time by Senior and by Bohren and Huffman [19,20], arriving at seemingly conflicting results and ascribing the spherical shape the minimal vs. the maximal absorption cross-section status, respectively. As was argued in [20], the discrepancy had to do with the chosen values of the dielectric constant. Polarizability has also been studied in material science where the emphasis is placed on effective properties of materials and mixture rules rather than on scattering. We note, in particular, a series of studies by Sihvola and colleagues [21–23], computing scalar

polarizabilities of platonic polyhedra and showing numerically that these exceed those of equal volume spheres.

Perhaps the earliest mention of the "spherical optimality" occurred in the mathematics literature in the late 1940s [24–26], resulting in the Polya–Szego conjecture regarding capacity and fluid-mechanical polarizability minima attained by spherical shapes. Note that, in contrast to this work, the Polya–Szego conjecture deals only with geometric entities. The conjecture has only recently been proven by mathematicians [27,28]. In the physics literature on capacitance, intrinsic conductivity and other "shape functionals" of conducting ellipsoids, e.g., see Fig. 1 of [29] and [30,31], also purely geometric quantities were considered. Below our emphasis is on simple examples of the interplay between electric and geometric contributions.

Our heuristic chain of reasoning is as follows. Among all ellipsoidal particles of equal volume, for reasons symmetry, it is likely that spherical shape is the one attaining extrema, say, in the orientation-averaged magnitude of the induced dipole moment. Also, ellipsoidal particles are the only ones whose internal fields are uniform albeit not necessarily aligned with the external electric field (the Eshelby conjecture [27]). On the other hand, Laplace's equation $\nabla^2\phi=0$ can be derived from the minimum of the volume integral squared gradient $\int_V|\nabla\phi|^2\,dV$. This suggests that any field gradients, and, in particular, field singularities near edges and corners, tend to increase the volume integral, causing non-ellipsoidal particles to have larger polarizabilities than equal volume ellipsoids of the same aspect ratio. Indeed, all numerical evidence we encountered so far lends support to this view, e.g., the correlation of Platonic solid polarizabilities with the number of faces, reported in [21].

Returning to electromagnetic scattering theory, we shall deal with a total *orientation-averaged* cross-sections of ellipsoidal particles, motivated by the high frequency region but focusing on the low frequency region, with an eye toward practical bounds for all size parameters [32]. En route, we consider shape optimality for orientation-averaged polarizabilities and magnitudes of an induced dipole moment. In particular, we examine the electrostatics case as a stand-alone problem, establishing optimality of the spherical bound and extending the discussion to the case of coated triaxial ellipsoids. We also study the dependence on the aspect ratio and the dielectric constant and disentangle geometrical effects (larger specific surface area) from the electric ones, e.g., conducting ellipsoids (infinite dielectric constant) are treated vis-a-vis dielectric and geometric ones. We use Taylor expansions in the dielectric contrast and in eccentricity to gain further physical insight. We also raise the question of the extent of size parameters to which spherical optimality holds. To that end, we use the T-matrix method to examine the range of validity of the spherical optimality vs. the size parameter for a variety of dielectric constants and aspect ratios.

2. Optimality of the spherical shape

Within the framework of electrostatics, what is the particle shape that attains minimal orientation-averaged magnitude of the induced dipole moment, while keeping volume (mass) and the dielectric function fixed? To that end, let us consider ellipsoidal particles. Let the three principal axes of a dielectric ellipsoid be along x, y and z directions. We shall use an analytic solution in the notation as given in Bohren and Huffman [33] but "renormalized" so that the vacuum permittivity is set to unity (see also [34,35]). When the ellipsoid is placed in external electric field $\vec{E}=E_1\hat{x}+E_2\hat{y}+E_3\hat{z}$, components of the induced dipole moment of the ellipsoid are given as follows ($\varepsilon_r=$ relative permittivity):

$$p_i=4\pi abc\frac{\varepsilon_r-1}{3+3L_i(\varepsilon_r-1)}E_i \tag{1}$$

where a, b and c are the principal semi-axes, and L_is are the associated depolarization coefficients of the dielectric ellipsoids as given, e.g., in [33,34].

For the special cases of prolate and oblate spheroids, the depolarization factors are given by

$$L_1=L_2=\frac{g(e)}{2e^2}\left[\frac{\pi}{2}-\tan^{-1}g(e)\right]-\frac{g^2(e)}{2},$$
$$L_3=1-2L_1 \tag{2}$$

where $g(e)=((1-e^2)/e^2)^{1/2}$.

$$L_1=\frac{1-e^2}{e^2}\left(-1+\frac{1}{2e}\log\frac{1+e}{1-e}\right),$$
$$L_2=L_3=\frac{(1-L_1)}{2} \tag{3}$$

Then, the associated polarizabilities are given by, e.g., Eq. 5.32 of [33]:

$$\alpha_i=4\pi abc\frac{\varepsilon_r-1}{3+3L_i(\varepsilon_r-1)}, \tag{4}$$

and the orientation-averaged polarizability is

$$\alpha=\frac{4\pi abc}{3}(\varepsilon_r-1)\frac{1}{3}\sum_{i=1}^{3}\frac{1}{1+L_i(\varepsilon_r-1)} \tag{5}$$

while the orientation-averaged polarizability, *normalized* per volume (α_n), is

$$\alpha_n=(\varepsilon_r-1)\frac{1}{3}\sum_{i=1}^{3}\frac{1}{1+L_i(\varepsilon_r-1)} \tag{6}$$

The coefficient of (1/3), arising from orientation averaging, merits an explanation. Polarizability is a 2nd rank tensor, linking the external electric field and the induced dipole moment vectors. Eq. (1) above is a special (diagonal) case, written in the principal axes of the ellipsoid. Orientation-averaged tensor is an isotropic one so its components do not change with coordinate rotations (there are rank 0 and 2 isotropic tensors but not rank 1). But 2nd rank isotropic tensor has the form $\alpha\mathbf{I}$ where $\mathbf{I}\equiv\mathrm{diag}(1,1,1)$ is the identity matrix and α is the orientation-averaged polarizability. One can find a by observing that the only scalar invariant at one's disposal is the tensor trace (Tr). As $Tr(\mathbf{I})=3$, (1/3) delivers normalization. The question of tensor isotropy is rather subtle in this context, as it yields *scalar* polarizabilities not only for a sphere but also for any 2nd rank isotropic tensor shapes such as Platonic polyhedra (see also somewhat cryptic remarks at the very conclusion of [21]). However, this is

not so for spheroids until orientation-averaging is performed.

To gain physical insight for the respective roles of geometry and electrostatics, we examine the transparent (Rayleigh–Gans) limit. To that end, define dielectric contrast as

$$\delta \equiv \varepsilon_r - 1 \tag{7}$$

We can rewrite the average polarizability per volume of dielectric ellipsoid in terms of δ. Then, upon expanding in Taylor series for $\delta \ll 1$ to $O(\delta^3)$, Eq. (6) yields the orientation-averaged polarizability per volume

$$\alpha_n \cong \frac{\delta}{3}\left[3-\delta(L_1+L_2+L_3)+\delta^2\left(L_1^2+L_2^2+L_3^2\right)\right] \tag{8}$$

Using the constraint

$$g(L_1,L_2,L_3) = L_1+L_2+L_3 = 1 \tag{9}$$

which holds for ellipsoids at all aspect ratios, we obtain

$$\alpha_n \cong \frac{\delta}{3}\left[3-\delta+\delta^2\left(L_1^2+L_2^2+L_3^2\right)\right] \tag{10}$$

which, for the sphere, reduces to $\alpha_{n,sphere} \cong (\delta/3)[3-\delta+\delta^2/3]$. We now introduce the spheroidal access as $\alpha_r \equiv \alpha_{n,spheroid}/\alpha_{n,sphere}$. Adding and subtracting $\delta^2/3$ in the numerator of α_r then yield the following equation:

$$\begin{aligned}\alpha_r &= 1+\frac{\delta^2(L_1^2+L_2^2+L_3^2-1/3)}{3-\delta+\delta^2/3}\\ &\approx 1+\frac{\delta^2(L_1^2+L_2^2+L_3^2-1/3)}{3}\end{aligned} \tag{11}$$

The separation of the geometrical $(L_1^2+L_2^2+L_3^2-1/3)$ and the electrical (δ^2) effects is now evident and appears to be a new insight. What shape attains minimal α_n? The question reduces to finding the minimum of $L_1^2+L_2^2+L_3^2$, subject to the constraint (9). A general proof is given below, but an appealing geometrical argument can now be given for spherical optimality, based on an isoperimetric inequality. Interpret the constraint (9) as a fixed perimeter of a rectangular solid, whose surface area, which is twice the quantity $L_1^2+L_2^2+L_3^2$, is the one to optimize. As the minimal surface area of all rectangular blocks of a given perimeter is that of a cube, i.e., $L_1=L_2=L_3=1/3$ in the space of depolarization factors, in real space the sphere delivers optimal shape. In the bottom panel (b) of Fig. 1, we illustrate this by plotting the logarithm of $\alpha_r = \alpha_{spheroid}/\alpha_{sphere} = 1+\delta^2(L_1^2+L_2^2+L_3^2-1/3)$.

For the special case of a conducting ellipsoid, components of the dipole moment are given by

$$p_i = \frac{E_i V}{4\pi L_i}, \tag{12}$$

where $i=1$, 2 and 3, V is volume of the ellipsoid and L_i is the depolarization coefficient of the conducting ellipsoid. Then, the polarizability is $\alpha_i = V/(4\pi L_i)$ and the orientation-averaged polarizability per volume is

$$\alpha_n = \frac{1}{12\pi}\left(\frac{1}{L_1}+\frac{1}{L_2}+\frac{1}{L_3}\right) \tag{13}$$

Coated particles are ubiquitous in applications, e.g., [36,37]. Next, we pose the optimal shape question about coated spheroids, apparently for the first time. Is the concentric spherical configuration still the optimal one? To that end, using the coated ellipsoid analytic solution, e.g., Eq. (5.35) in [33], we write the components of polarizability of a coated confocal ellipsoid as

$$\alpha_i = \frac{V\left((\varepsilon_2-1)\left[\varepsilon_2+(\varepsilon_1-\varepsilon_2)\left(L_i^{(1)}-fL_i^{(2)}\right)\right]+f\varepsilon_2(\varepsilon_1-\varepsilon_2)\right)}{\left[\varepsilon_2+(\varepsilon_1-\varepsilon_2)\left(L_i^{(1)}-fL_i^{(2)}\right)\right]\left[1+(\varepsilon_2-1)L_i^{(2)}\right]+fL_i^{(2)}\varepsilon_2(\varepsilon_1-\varepsilon_2)} \tag{14}$$

where V is total volume of the ellipsoid, f is the ratio of volume of inner ellipsoid per total volume, ε_1 and ε_2 is the relative permittivity of the inner and outer ellipsoids, superscript (1) and (2) denotes inner and outer, respectively. Then, the orientation-averaged polarizability per volume of the coated ellipsoid is

$$\alpha_n = \frac{1}{3}\sum_{i=1}^{3}\frac{\left((\varepsilon_2-1)\left[\varepsilon_2+(\varepsilon_1-\varepsilon_2)\left(L_i^{(1)}-fL_i^{(2)}\right)\right]+f\varepsilon_2(\varepsilon_1-\varepsilon_2)\right)}{\left[\varepsilon_2+(\varepsilon_1-\varepsilon_2)\left(L_i^{(1)}-fL_i^{(2)}\right)\right]\left[1+(\varepsilon_2-1)L_i^{(2)}\right]+fL_i^{(2)}\varepsilon_2(\varepsilon_1-\varepsilon_2)} \tag{15}$$

Results of our calculations for polarizabilities of dielectric, conducting, transparent and coated confocal ellipsoids vs. the (inner) aspect ratio ρ are shown in the two panels of Fig. 1. Along with the evident spherical optimality, they also include the monotonic dependence on the aspect ratio. Also shown, for comparison, is the relative spheroidal surface area. It can now be readily understood why the geometric case is the intermediate one between the conducting and the dielectric one: as the relative permittivity approaches unity, spheroidal excess disappears at all aspect ratios. Note that the results hold for confocal coated spheroids, regardless of the sign of $\delta\varepsilon = \varepsilon_2-\varepsilon_1$ (Fig. 3).

In passing, we note that the minimum at the spherical value of $\rho=1$ is smooth for all curves so that in the near-spherical expansion, the first non-zero term in the aspect ratio is quadratic. Also, note that no qualitative change in the plot would occur, if one were to move from ρ to $\delta\rho$, defined by $\rho = 1+\delta\rho$ and subtract off unity from all abscissa values. Now, quadratic dependence in $\delta\rho$ implies 4th order dependence in eccentricity as $e \approx [2(\rho-1)]^{1/2}$ (we used the prolate expression as an example). Calculations show that this is, indeed, the case, e.g., eccentricity expansions of the relative surface area of oblate and prolate spheroids, respectively, are $O(e^4)$ and contain even powers as follows:

$$S_r \cong 1+\frac{2e^4}{45}+\frac{136e^6}{2835}+\frac{131e^8}{2835}+\frac{12224e^{10}}{280665}+\cdots \tag{16}$$

$$S_r \cong 1+\frac{2e^4}{45}+\frac{116e^6}{2835}+\frac{101e^8}{2835}+\frac{8764e^{10}}{280665}+\cdots \tag{17}$$

We now proceed to the scattering cross-sections. As the orientation-averaged absorption cross-sections scale with the product of the imaginary part of relative permittivity and the arithmetic average of principal polarizabilities (e.g., see Eq. (1) and Eq. (5.44) of [20,33], respectively), shape optimization proceeds exactly as for polarizabilities. Therefore, we next consider the orientation-averaged scattering cross-section, given by (e.g., Eq. (5.45) in [33])

$$\langle C_{sca}\rangle = \frac{k^4}{18\pi}\left(|\alpha_1|^2+|\alpha_2|^2+|\alpha_3|^2\right) \tag{18}$$

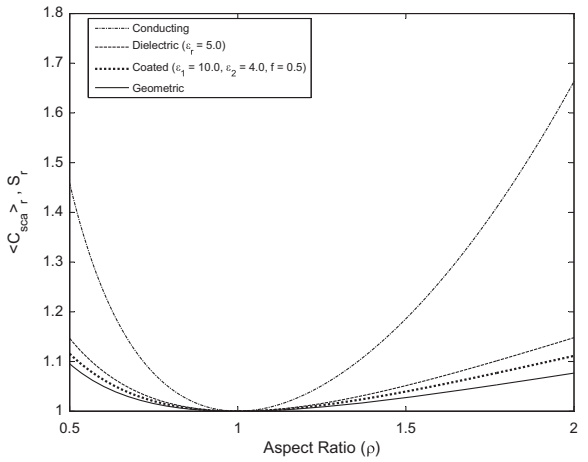

Fig. 2. Optimality of the spherical shape: scattering cross-sections. Plotted are dielectric, conducting, and confocal coated spheroid scattering cross-sections vs. the aspect ratio. Also plotted for comparison is relative (normalized by equal-volume-sphere values) surface area S_r. The curves labels identical to Fig. 1. Optimality of the spherical shape is evident in all cases.

Substituting for the polarizability from Eq. (4) into the above equation, we obtain

$$\langle C_{sca}\rangle = \frac{k^4(4\pi abc)^2(\varepsilon_r-1)^2}{18\pi}\sum_{i=1}^{3}\left[\left(\frac{1}{1+L_i(\varepsilon_r-1)}\right)^2\right] \tag{19}$$

Similarly, substituting the polarizability of a conducting ellipsoid in Eq. (18), for the scattering cross section of conducting ellipsoid we obtain

$$\langle C_{sca}\rangle = \frac{k^4V^2}{288\pi^2}\left(\frac{1}{L_1^2}+\frac{1}{L_2^2}+\frac{1}{L_3^2}\right) \tag{20}$$

For the coated ellipsoid case, the average scattering cross section is

$$\langle C_{sca}\rangle = \frac{k^4V^2}{18\pi}\sum_{i=1}^{3}\left(\frac{(\varepsilon_2-1)\left[\varepsilon_2+(\varepsilon_1-\varepsilon_2)\left(L_i^{(1)}-fL_i^{(2)}\right)\right]+f\varepsilon_2(\varepsilon_1-\varepsilon_2)}{\left[\varepsilon_2+(\varepsilon_1-\varepsilon_2)\left(L_i^{(1)}-fL_i^{(2)}\right)\right]\left[1+(\varepsilon_2-1)L_i^{(2)}\right]+fL_i^{(2)}\varepsilon_2(\varepsilon_1-\varepsilon_2)}\right)^2 \tag{21}$$

The results are plotted in Fig. 2 and spherical optimality is evident once more. We have been able to prove spherical optimality of polarizabilities and cross-sections for the conducting and dielectric spheroids. We use dielectric ellipsoid family to illustrate the proof by employing the method of Lagrange multipliers.

Consider the space of depolarization factors, spanned by L_1, L_2 and L_3. While varying ellipsoidal shapes, the relative permittivity is held constant and the objective function is

$$F(L_1,L_2,L_3) = \sum_{i=1}^{3}\frac{1}{1+L_i(\varepsilon_r-1)} \tag{22}$$

with the constraint in (9). Following the method of Lagrange multipliers, we write

$$\vec{\nabla}F(L_1,L_2,L_3) = \lambda\vec{\nabla}g(L_1,L_2,L_3) \tag{23}$$

Then, we get

$$\frac{\partial}{\partial L_i}\frac{1}{1+L_i(\varepsilon_r-1)} = \lambda \tag{24}$$

for $i=1,2,3$. Insofar as this Equation is invariant w.r.t. interchange of labels, that is, completely symmetric in L_1, L_2, and L_3, it follows that $L_1=L_2=L_3$ delivers the minimum and $L_i=1/3$ is obtained from the constraint (9). This represents spherical depolarization factors. We used the same method to establish spherical optimality for Eqs. (13), (19) and (20). We used the MATLAB numerical optimization program 'Genetic Algorithm' to find the aspect ratio of the inner spheroid, leading to the minimum in orientation-averaged polarizability and scattering cross-section of confocal coated spheroids. The optimization was performed by setting the pairs of relative permittivities of inner and outer ellipsoids $(\varepsilon_1,\varepsilon_2)$ as $\{1.1, 1.5, 2.0, 2.1, 4, 10, 99.5, 100.0\}$. The values of ε_1 and ε_2 span the cases: (1) $\varepsilon_1<\varepsilon_2$, (2) $\varepsilon_1>\varepsilon_2$, (3) $\varepsilon_1\approx\varepsilon_2$, (4) $\varepsilon_1,\varepsilon_2\gg 1$ and (5) $\varepsilon_1,\varepsilon_2\to 1$ and thus include all essential possibilities. Moreover, we set the volume fraction of the inner to the total ellipsoid as $1/5, 1/2, 4/5$ in order to test the thick, intermediate and thin shell cases. The numerical results confirmed that minimum in orientation-averaged polarizability and cross section occurs at the spherical shape.

We note that symmetry arguments suggest spherical optimality for coated particles; coated sphere attains minimum numerically as Fig. 3 illustrates. The surprise is that upon switching the sign of $(\varepsilon_1-\varepsilon_2)$, orientation-averaged polarizability value of the coated sphere does not flip from minimum to maximum. Taking the limit of empty interior $(\varepsilon_1=1)$ and using superposition for cavities help with interpretation via dielectric shell configurations. However, symmetry arguments may not hold for the general case of coated ellipsoids of arbitrary relative orientation.

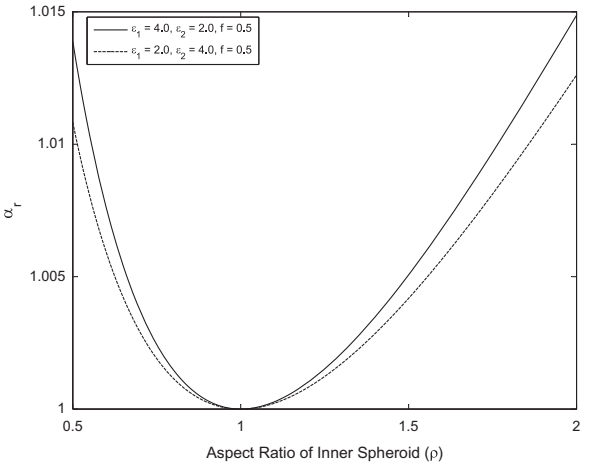

Fig. 3. Optimality of the coated spherical shape: orientation-averaged polarizability, α_r of a spheroid, coated by a sphere vs. the aspect ratio of inner spheroid. Two polarizability curves are shown, representing the cases $\epsilon_1<\epsilon_2$ (dashed line) and $\epsilon_1>\epsilon_2$ (solid line).

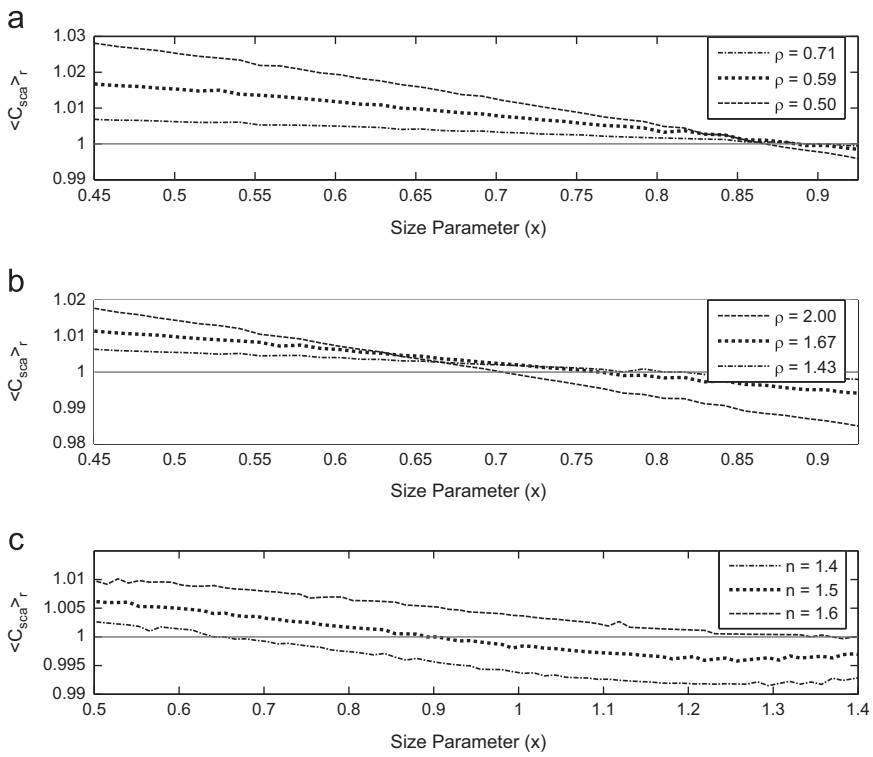

Fig. 4. Scattering cross-section vs. the size parameter ka where k is the wave-number and a is the radius of the equal volume sphere. The top (oblate) and middle (prolate) panels show, for various values of the aspect ratio ρ but constant refractive index $n=1.5$, that randomly oriented spheroids begin to drop below the spherical value at size parameters such that the particle diameter is about a third or a quarter of the incident wavelength. The bottom panel presents the case of scattering by randomly oriented spheroids with a fixed aspect ratio $\rho=0.71$ for three different values of the refractive index.

3. Spherical optimality beyond the Rayleigh region

Having established the optimality of the spherical shape in the low frequency regime and having discussed it in the high frequency regime, one is naturally tempted to bridge it for all size parameters. However, the underlying physics renders it unlikely as resonances occur in the intermediate region and spheroids are, in fact, known to scatter less than spheres at some size parameters. One may still hope that such a region is not wide when orientation-averaged properties of spheroids are compared to those of equivalent sphere and that in most practical applications natural size distributions wash out the resonances. As a first step toward this goal, we used the T-matrix method to get a feel for the extent of the range within which the spherical optimality holds. For example, at what size parameter does the relative cross-section drop below unity and ellipsoidal superiority ceases? To that end, we computed the scattering cross-section for a randomly oriented spheroids relative to one for equivalent volume spheres.

The results are shown in the three panels of Fig. 4. All the three panels show scattering cross-section vs. the size parameter ka where k is the wave-number and a is the radius of the equal volume sphere. The top (oblate) and middle (prolate) panels show, for various values of the aspect ratio ρ, that randomly oriented spheroids begin to drop below the spherical value at size parameters such that the particle diameter is about a quarter of the incident wavelength. This seems reasonable as scattering from parts of the particle can exhibit interference at these parameters. The bottom panel presents the case for three different values of the refractive index for randomly oriented spheroids at a fixed aspect ratio. It is observed that stronger dielectric effects (larger dielectric constant) take longer to drop down to the spherical value in the size parameter space and the crossing occurs on the order of size parameter of unity. Note that while the effect looks small ($\sim 3\%$) for the chosen index of refraction and aspect ratios, for this figure and for the other figures throughout this paper, we obtained much larger effects for large aspect ratios and large dielectric constants.

Recalling that spherical optimality holds at the high end (large particles) down to the size parameter of ~ 10 [7] and at the low end (small particles) up to size parameter ~ 1, suggests that the intermediate region is not overwhelmingly broad and that even narrow distributions of sizes may wash out the resonances, thereby rendering spherical optimality broadly valid. Systematic investigation of this conjecture is beyond the scope of this paper but will be a subject of future work.

4. Concluding remarks

The question of optimal shape, e.g., that causing minimal extinction among all shapes of equal volume, has been examined. We focused on the low frequency approximation for ellipsoids, elucidating the roles of electric and

geometric contributions and giving a simple proof of spherical optimality for a ellipsoidal particle. Monotonic increase with asphericity in the low frequency regime for orientation-averaged induced dipole moments and scattering cross-sections has been discussed. Even a stand-alone remark in electrostatics that a sphere has the least orientation-averaged dipole moment of all randomly oriented particles of equal volume, merits a footnote in any text on electromagnetism, in authors opinion. We also propose to bridge low and high frequency regimes in a single minimum principle throughout the range of size parameters, given realistic size distributions of randomly oriented aspherical particles. A sceptical reader might object that most of the above considerations have been confined to the ellipsoidal group. We now suggest another argument for the generality of the spherical optimum, based on the sum rule for integrated extinction, and then return to arbitrary particle shapes.

Consider the extinction cross-section, integrated over all wavelengths. By dimensional analysis, the result has units of volume. Thus, once the question is asked, one might expect the result to depend on particle volume as the only characteristic length scales in the problem are particle size (a) and the wavelength λ but the latter is integrated out. In [38], Purcell derived the following integrated extinction result (see Eq. 4.81 in [33] for this particular way of writing it):

$$\int_0^\infty C_{ext}(\lambda)\, d\lambda = 4\pi^3 a^3 \left(\frac{\varepsilon(0)-1}{\varepsilon(0)+2}\right) \tag{25}$$

for a spherical particle. Remarkably, the integrated extinction involves only the static dielectric constant, arising from using Kramers–Kronig relation in the derivation of [38]. For randomly oriented spheroidal particles, the integrated extinction has the same form as Eq. (25) but with the pre-factor which depends on the depolarization factors [38], L_i as throughout this paper. By symmetry arguments, again, the sphere has least integrated extinction among all ellipsoidal particles. This suggests that in the integrated sense, spheres will be minimal, with ellipsoids causing a bit more extinction and other shapes of equal volume and aspect ratio, likely higher.

Why do we suspect that other shapes of equal volume are likely to exceed ellipsoids? First, there is the numerical evidence. The relative orientation-averaged polarizability of icosahedron, dodecahedron, octahedron, cube and tetrahedron with relative permittivity $\varepsilon_r = 5.0$ are 1.0147, 1.0207, 1.0538, 1.0661 and 1.1454, respectively [21]. Secondly, according to the weak Eshelby conjecture, ellipsoids are the only particle shapes able to contain a uniform electric field in their interiors [27] albeit not necessarily aligned with the external electric field. The converse is also true (strong Eshelby conjecture, e.g., see [39]). On the other hand, as discussed in the Introduction, it was suggested that any gradients and field singularities tend to increase the volume integral, causing non-ellipsoidal particles to have larger polarizabilities, etc., than those of equal volume ellipsoids of comparable aspect ratio. Note that one has to exercise caution when comparing ellipsoids to polyhedra or finite cylinders because of fundamentally different limits of aspect ratio. Ellipsoids are deformed spheres and convert to spheres at $\rho = 1$ but this is not so for cubes, finite circular cylinders, tetrahedra, etc.

It is an interesting fact that the polarizability tensor reduces to a scalar (multiple of an identity matrix) not only for spheres but for any particle possessing three mutually orthogonal and identical symmetry axes, e.g., platonic polyhedra. As an isotropic tensor is also of this form, no orientation-averaging is necessary when examining low frequency scattering of such particles. While regular polyhedra lack complete rotational symmetry to fit, say, a T-matrix method, they nevertheless supply comparable computational advantage for small size parameters, at least, as only a single orientation has to be computed. As an important possible application of the above seemingly academic consideration, consider modelling and remote sensing of fine dust. A micron size particle is just the right size to interact strongly with visible and thermal radiation but it is also just the right size to stay aloft for days because it falls in a laminar regime, greatly sensitive to particle shape. In this sedimentation problem the role of the polarizability tensor is played by the resistance tensor of microhydrodynamics. For the reasons of tensor symmetry, identical to just discussed above, regular polyhedra have the resistance tensor which is a multiple of an identity matrix [40]. This has the surprising consequence that, say, cubes or tetrahedrons fall at the same speed, regardless of orientation. Hence, modelling of, say, Saharan dust for remote sensing purposes could be based on regular polyhedra and variable aspect spheroids without significant loss of generality.

Acknowledgments

This work was supported by the NSF Grant AGS-111916. We wish to thank Gregory Ryskin, Sarah Kostinski, and Elizabeth Chen for useful comments and Michael Mishchenko for directing us to T-matrix Fortran computer codes, publicly available at http://www.giss.nasa.gov/staff/mmishchenko/t_matrix.html.

References

[1] Mishchenko MI, Hovenier JW, Travis LD. Light scattering by nonspherical particles: theory, measurements, and applications. Academic Press; 1999.
[2] Dubovik O, Sinyuk A, Lapyonok T, Holben BN, Mishchenko M, Yang P, et al. Application of spheroid models to account for aerosol particle nonsphericity in remote sensing of desert dust. J Geophys Res Atmos 2006;1984–2012:111.
[3] Dubovik O, Herman M, Holdak A, Lapyonok T, Tanre D, Deuze JL, et al. Statistically optimized inversion algorithm for enhanced retrieval of aerosol properties from spectral multi-angle polarimetric satellite observations. Atmos Meas Tech 2011;4:975–1018.
[4] Koch AL, Ehrenfeld E. The size and shape of bacteria by light scattering measurements. Biochim Biophys Acta Gen Subj 1968;165:262–73.
[5] Van De Hulst HC. Light scattering by small particles (structure of matter series), 2010.
[6] Lehahn Y, Koren I, Boss E, Ben-Ami Y, Altaratz O. Estimating the maritime component of aerosol optical depth and its dependency on surface wind speed using satellite data. Atmos Chem Phys 2010;10:6711–20.
[7] Chylek P. Extinction cross sections of arbitrarily shaped randomly oriented nonspherical particles. J Opt Soc Am 1977;67:1348–50.

[8] Pollack JB, Cuzzi JN. Scattering by nonspherical particles of size comparable to wavelength—a new semi-empirical theory and its application to tropospheric aerosols. J Atmos Sci 1980;37:868–81.
[9] Krotkov NA, Flittner D, Krueger A, Kostinski A, Riley C, Rose W, et al. Effect of particle non-sphericity on satellite monitoring of drifting volcanic ash clouds. J Quant Spectrosc Radiat Transfer 1999;63:613–30.
[10] Siegel KM. Far field scattering from bodies of revolution. Appl Sci Res, 1958 293–328.
[11] Haywood J, Johnson B, Osborne S, Mulcahy J, Brooks M, Harrison M, et al. Observations and modelling of the solar and terrestrial radiative effects of Saharan dust: a radiative closure case study over oceans during the GERBILS campaign. Q J R Meteorol Soc 2011;137:1211–26.
[12] Asano S, Yamamoto G. Light scattering by a spheroidal particle. Appl Opt 1975;14:29–49.
[13] Asano S. Light scattering properties of spheroidal particles. Appl Opt 1979;18:712–23.
[14] Goncharenko A, Venger E, Zavadskii S. Effective absorption cross section of an assembly of small ellipsoidal particles. J Opt Soc Am B 1996;13:2392–5.
[15] Goncharenko A, Semenov YG, Venger E. Effective scattering cross section of an assembly of small ellipsoidal particles. J Opt Soc Am A 1999;16:517–22.
[16] Goncharenko A, Popelnukh V, Venger E. Effect of weak nonsphericity on linear and nonlinear optical properties of small particle composites. J Phys D Appl Phys 2002;35:1833.
[17] Moosmller H, Chakrabarty R, Arnott W. Aerosol light absorption and its measurement: a review. J Quant Spectrosc Radiat Transfer 2009;110:844–78.
[18] Atlas D, Kerker M, Hitschfeld W. Scattering and attenuation by nonspherical atmospheric particles. J Atmos Terr Phys 1953;3:108–19.
[19] Senior T. Effect of particle shape on low frequency absorption. Appl Opt 1980;19:2483–5.
[20] Bohren CF, Huffman DR. Absorption cross-section maxima and minima in IR absorption bands of small ionic ellipsoidal particles. Appl Opt 1981;20:959–62.
[21] Sihvola A, Yla-Oijala P, Jarvenpaa S, Avelin J. Polarizabilities of platonic solids. IEEE Trans Antennas Propag 2004;52:2226–33.
[22] Sihvola A. Dielectric polarization and particle shape effects. J Nanomater 2007:5.
[23] Venermo J, Sihvola A. Dielectric polarizability of circular cylinder. J Electrostatics 2005;63:101–17.
[24] Polya G, Szego G. Inequalities for the capacity of a condenser. Am J Math 1945;67:1–32.
[25] Polya G. A minimum problem about the motion of a solid through a fluid. Proc Natl Acad Sci USA 1947;33:218.
[26] Jones D. Low frequency electromagnetic radiation. IMA J Appl Math 1979;23:421–47.
[27] Kang H, Milton GW. Solutions to the Polya–Szego conjecture and the weak Eshelby conjecture. Arch Ration Mech Anal 2008;188:93–116.
[28] Kang H. Conjectures of Polya–Szego and Eshelby, and the Newtonian potential problem: a review. Mech Mater 2009;41:405–10.
[29] Garboczi E, Snyder K, Douglas J, Thorpe M. Geometrical percolation threshold of overlapping ellipsoids. Phys Rev E 1995;52:819.
[30] Douglas JF, Garboczi EJ. Intrinsic viscosity and the polarizability of particles having a wide range of shapes. Adv Chem Phys 1995;91:85–154.
[31] Garboczi E, Douglas J. Intrinsic conductivity of objects having arbitrary shape and conductivity. Phys Rev E 1996;53:6169.
[32] Bi L, Yang P, Kattawar GW, Kahn R. Single-scattering properties of triaxial ellipsoidal particles for a size parameter range from the Rayleigh to geometric-optics regimes. Appl Opt 2009;48:114–26.
[33] Bohren CF, Huffman DR. Absorption and scattering of light by small particles. Wiley; 1983.
[34] Landau LD, Lifshitz EM. Electrodynamics of continuous media. Oxford: Pergamon Press; 1960.
[35] Stratton JA. Electromagnetic theory. McGraw-Hill Book Company; 1941.
[36] Erlick C. Effective refractive indices of water and sulfate drops containing absorbing inclusions. J Atmos Sci 2006;63:754–63.
[37] Voshchinnikov NV. Electromagnetic scattering by homogeneous and coated spheroids: calculations using the separation of variables method. J Quant Spectrosc Radiat Transfer 1996;55:627–36.
[38] Purcell EM. On the absorption and emission of light by interstellar grains. Astrophys J 1969;158:433–40.
[39] Moroz A. Depolarization field of spheroidal particles. J Opt Soc Am B 2009;26:517–27.
[40] Kim S, Karrila SJ. Microhydrodynamics: principles and selected applications. Courier Dover Publications; 1991.